NANO LETTERS

2008
Vol. 8, No. 1
287−293

Solution Control of Radiative and Nonradiative Lifetimes: A Novel Contribution to Quantum Dot Blinking Suppression

Vasiliy Fomenko and David J. Nesbitt*

JILA, National Institute of Standards and Technology and University of Colorado, Department of Chemistry and Biochemistry, University of Colorado, Boulder, Colorado 80309

Received October 15, 2007; Revised Manuscript Received November 17, 2007

ABSTRACT

Time-correlated single photon counting methods are used with confocal microscopy and maximum likelihood estimation analysis to obtain fluorescence lifetime trajectories for single quantum dots with KHz update rates. This technique reveals that control of the solution environment can influence both radiative (k_{rad}) and nonradiative (k_{nonrad}) pathways for electron–hole recombination emission in a single quantum dot and provides a novel contribution mechanism to nearly complete suppression of quantum dot blinking, specifically by an increase in k_{rad}.

Introduction. A detailed understanding of the photophysical properties in semiconductor nanocrystals is of crucial importance for both fundamental research and nanotechnology applications.[1−10] The synthetic methods for growth of colloidal semiconductor nanocrystals have been extensively developed in the past two decades and now allow the size, shape, and dimensionality of the nanocrystals to be varied over a remarkably wide range.[11−17] This control over structure also permits the electronic and optical properties to be changed considerably. For example, the band edge fluorescence of nanocrystals can be tuned with size over the entire visible range, with extension into the near UV and near IR now routinely achieved.[18−23] Such combined control of structural and electronic/optical properties at the single quantum dot level provides an increasingly powerful tool for investigation and applications of semiconductor nanocrystals. Single-molecule fluorescence microscopy techniques have proven particularly important in revealing detailed photophysical dynamics that would otherwise be obscured in ensemble measurements. As two particularly relevant cases, single molecule studies have elucidated dramatic variation in fluorescence intensities of nanocrystals with time (fluorescence intermittency, or "blinking")[24−26] as well as spectral frequency shifting of the fluorescence maximum (spectral diffusion).[27−30]

A canonical picture for describing nanocrystal blinking phenonmena is based on the Auger model, whereby fluorescence intermittency is caused by fluctuations in net charge inside or around the nanocrystals.[3,5,26,31] Specifically, if photoexcitation results in an electron hole pair, there is a finite probability of either the electron or hole migrating to traps at the surface, leaving a delocalized charge in the nanocrystal core.[30,32] Subsequent photoexcitation of a second electron−hole pair in the charged dot leads to transient trion formation, which can decay via nonradiative Auger processes much faster than the intrinsic radiative rate. This results in a transient photophysical state of low quantum yield,[2,25] that can recover (i.e., "blink") by reentry of charge from the trap state into the nanocrystal. Such fluorescence blinking behavior depends on a variety of experimental conditions such as the thickness of the passivating inorganic shell, excitation intensity, and temperature.[27]

As a result of such trap state dynamics, one might anticipate that fluorescence fluctuations could be significantly affected by changes in the quantum dot environment.[33−38] For example, it was shown that the surrounding gas environment can influence the blinking dynamics for colloidal nanocrystals,[39] whereas InGaAs quantum dots grown epitaxially by the Stranski−Krastanow mechanism and embedded in solid GaAs (where the charge traps are relatively shallow), blink very infrequently at room temperature but start blinking[40] in the range of ∼10 K. In solution-phase studies, Ha and co-workers demonstrated reversible near-complete suppression of blinking at the single-molecule level by addition of millimolar amounts of thiols (β-mercaptoethanol, BME) to CdSe/ZnS dots encapsulated with polymer

* Author to whom correspondence should be addressed. E-mail: djn@jila.colorado.edu.

10.1021/nl0726609 CCC: $40.75
Published on Web 12/21/2007

and conjugated to streptavidin (Q-dots of Quantum Dot Corp.).[10] A follow-up ensemble study by Jeong et al.[9] showed that the effect of thiols on core-shell CdSe/ZnS blinking dynamics can be more complex, either increasing or decreasing the frequency of blinking. Specifically, the authors correlate such blinking suppression to the conjugate base thiolate ion, which in turn depends on pH and thiol exposure time. Recent work by Barnes and co-workers has demonstrated comparable suppression of blinking dynamics by addition of oligo phenylene vinylene ligands to bare CdSe quantum dots.[33,34] These studies each highlight the interesting and complex role of surface ligands in passivating surface traps states and producing stable, high quantum yield semiconductor quantum dots.

In this letter, time-correlated single photon counting methods are used to explore the effect of chemical environment on fluorescence lifetime, which in turn dramatically influences the fluorescence blinking dynamics. We demonstrate that chemical modification of the quantum dot environment can significantly change both the radiative (k_{rad}) and nonradiative (k_{nonrad}) rates, which can result in nearly complete suppression of blinking. Specifically, the data indicate as much as a 5-fold increase in the radiative rate for excitonic CdSe/ZnS core-shell nanocrystal emission with changes in the solution environment, accompanied by a reduction in the nonradiative relaxation pathways. This highlights a novel contribution to blinking suppression, namely competition with quantum dot nonradiative loss pathways by an environmentally induced *increase* in the radiative rate.

Methods. The experimental setup consists of a confocal scanning microscope coupled with fast pulsed-diode excitation and single photon detection. The excitation light is expanded by telescope before entering the microscope to achieve optimal diffraction-limited focusing conditions. An oil-immersion objective (100× magnification, 1.4 NA) is used to focus the light on a sample and to collect the sample fluorescence. A dichroic mirror both couples the diode laser into the objective as well as separates fluorescence and excitation light. The fluorescence collected by the objective is focused through a 50 μm pinhole, further split into two by a polarization beam splitter and imaged with 1:1 magnification on a pair of avalanche photodiodes (APD SPCM-AQR14, Perkin-Elmer).[41] Band-pass interference (Omega Optical, 550WB150) filters are used to allow the fluorescence to pass to the detectors and to suppress the light outside of the QD fluorescence band.

Excitation at 434 nm is provided by a GaN diode laser (LDH 440, PicoQuant) with a pulse width of about 70 ps, repetition rate between 2.5 and 40 MHz, and typical laser powers of ≈100 nW at the focus of the microscope objective. Single photon counting is performed with a time-correlated counter incorporated in a PC card (TSPC-134, Becker-Hickl). Time-correlated, time-tagged fluorescence measurements allow measurement of both the time between excitation pulse and photon emission (τ_{micro}) and the photon arrival time since the start of the experiment (τ_{macro}). Streptavidin-conjugated CdSe/ZnS quantum dots are obtained from Q-dots, Inc. with

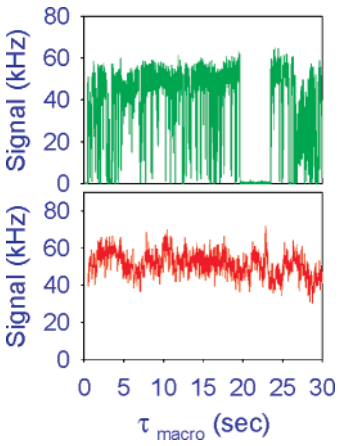

Figure 1. Fluorescence trajectories for single tethered CdSe/ZnS conjugates in $NaBO_2$ buffer (top panel) and in $NaBO_2$ buffer + 12 mM propyl gallate (bottom panel). Note the nearly complete suppression of blinking without change in fluorescence quantum yield.

mean core diameters of ∼4 nm and an estimated ZnS coating of a few monolayers. The samples were prepared for single molecule studies by tethering the streptavidin-conjugated QDs to biotin-modified glass slides in a microfluidic channel sample holder. The cleaning procedure for glass cover slips involved two stages: immersion in HNO_3 for 8−10 h and ozone-cleaning for at least 1.5 h but no more than 4 h prior to sample preparation. The studies of CdSe/ZnS samples are all performed at room temperature.

Microfluidic Control of Blinking Suppression. Surface-tethered quantum dots in sodium borate buffer (pH = 9.0) demonstrate pronounced blinking behavior (e.g., see upper panel of Figure 1), as noted in extensive studies by several groups.[2,9,10,25−27,30−32,39,42−44] A standard model for such an abrupt loss of fluorescence quantum yield is ionization of the QD, formed either by (i) rapid Auger relaxation of the biexciton or (ii) tunneling/thermally activated ejection of either electron or hole to surface traps. The presence of such trap states external to the quantum dot therefore offers an appealing mechanism for influencing the blinking dynamics by modification of the surface environment.[29,30,33,34,45]

The present study of blinking suppression dynamics is based on introduction of a dilute (0−15 mM) propyl gallate (3,4,5-trihydroxybenzoic acid propyl ester) solution to single quantum dots using a simple microfluidic pump syringe system. Solutions of both propyl gallate and quantum dots are first subjected to initial deoxygenation by bubbling Ar gas through a 1 mL solution for 20 min. Such inoculation with propyl gallate leads to a dramatic suppression of blinking behavior, as demonstrated for a single quantum dot fluorescent trajectory in the lower panel of Figure 1. Note that the vertical scale for upper and lower panels are the same, as well as the conditions of laser excitation and fluorescence collection. Thus, the peak count rates for the quantum dot remain nearly identical (50(4) and 52(6) KHz) in the absence or presence of the propyl gallate solution. It is worth noting that this behavior is not unique to propyl gallate; we have observed solution-based modification to

quantum dot blinking dynamics for a number of simple ligands, which will be reported elsewhere.

In an independent experiment, we have also quantified our microscope apparatus with detailed real time fluorescence correlation studies[46−48] (FCS) on dilute solutions (100 pM) of Alexa 430 dye molecules. Alexa 430 is used for better spectral match to the diode laser with its quantum yield (74% at 434 nm) measured independently by fluorimetric comparison with the well studied Rhodamine 6G. The lateral excitation beam profile at the focus can be independently confirmed by scanning over single dye molecules spin-coated on a coverslip, which in conjunction with the absorption cross section and quantum yield of Alexa 430 in solution, the number of confocal emitters (N) and measured laser power at the focus yields the rate of single molecule photoemission, dN^*/dt and translates into a microscope collection efficiency of 3.25%. Collection efficiency can also be confirmed by measuring fluorescence intensities for solution-phase Alexa 430 dye molecules tethered to the surface. This in turn permits accurate determination of absolute quantum yields for quantum dots tethered to the coverglass surface, based on known QD absorption cross sections and measured laser excitation powers (typically ≈100 nW). Such an analysis indicates peak (i.e., "on") quantum yields for the nanocrystal samples of ≈ 80% or higher with quantum yields decreasing to <1−2% in the "off" state. What is crucial is that the observed count rates are linearly proportional to the fluorescence quantum yield; thus observation of the same peak emission rate with and without propyl gallate implies that blinking suppression is achieved with little or no change in peak quantum yield.

As propyl gallate is a known oxygen scavenger, one might first suspect that the presence or absence of O_2 is responsible for blinking suppression.[39] Indeed, there are studies that suggest O_2 removal of electrons from trap states as a potential mechanism in both nanocrystals and bulk semiconductors. To address this issue, we have performed a series of control experiments with alternative oxygen removal techniques, specifically thorough degassing of the solutions with He, Ar, and efficient biochemical scavenging of O_2 with glucose oxidase catalase.[49] These studies indicate that oxygen removal by itself does not result in any noticeable suppression of blinking dynamics. Thus, we conclude that changes in the nanocrystal blinking dynamics arise primarily by contact with propyl gallate itself.

Fluorescence Lifetime Trajectories. To gain physical insight into the quantum dot blinking suppression behavior, we have performed correlated fluorescence lifetime and intensity measurements on many (>50) propyl gallate-treated and -untreated quantum dots. The time-tagged, time-resolved singe photon counting capabilities allow both fast time delay (micro) and wallclock (macro) information to be stored for each detected photon. Thus, the detected photons can be analyzed in groups (typically 50−100 photons each) as a function of time along the fluorescence trajectory. Estimates of fluorescence lifetimes for each group are carried out using maximum likelihood estimator methods (MLE).[50−52] To enhance the dynamic fitting range for the exponential decays,

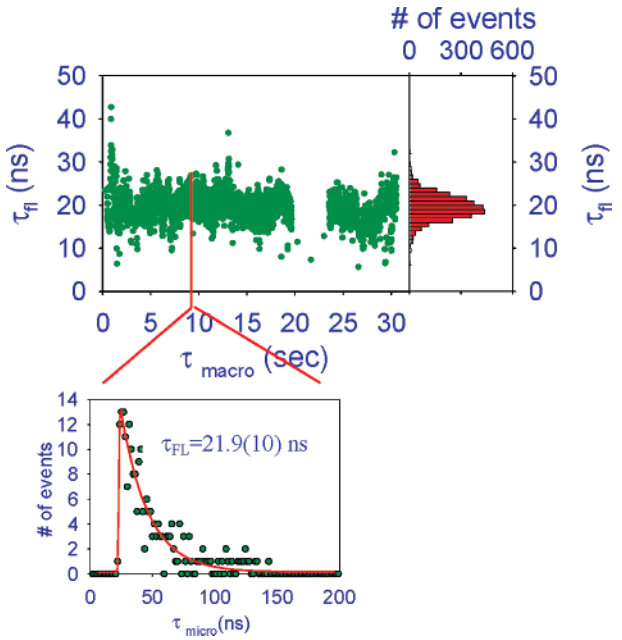

Figure 2. Upper left panel: Typical fluorescence lifetime trajectory for a single CdSe/ZnS quantum dot in $NaBO_2$ buffer in the absence of propyl gallate solution. Each fluorescence lifetime is obtained by fitting 100 photon events to a single-exponential decay with a maximum likelihood estimator algorithm. Lower panel: A data slice near τ_{macro} = 9.50 s from which a sample τ_{micro} = 21.9(10) ns fluorescence lifetime is extracted.

we have further modified the MLE equations to take into account a small background offset due to random photon arrival. At 60 kHz count rates and 50−100 photons per group (Figure 2, lower panel), this translates into a typical fluorescence lifetime update rate of 0.6 −1.2 kHz. Such MLE analysis of the quantum dot data in Figure 1 (upper panel) yields the fluorescence lifetime (τ_{Fl}) trajectory shown in Figure 2 (upper panel) and an average lifetime of $<\tau_{Fl}> \approx$ 21(1) ns. Further experiments show that these lifetimes are independent of laser excitation power, which has been varied from 200 W/cm^2 to 4.25 kW/cm^2 (approximately 50 nW to 1.0 μW average power).

The key result featured in this report is the remarkable change in the fluorescence lifetimes observed in the presence of propyl gallate. Specifically, Figure 3 illustrates that blinking suppression is accompanied by a strong 5-fold reduction in fluorescence lifetime from $<\tau_{Fl}>$ = 21(1) ns down to $<\tau_{Fl}>$ = 4(1) ns. This dramatic reduction in fluorescence lifetime is quite reproducible, which we have confirmed in studies of multiple samples and quantum dots. Furthermore, both the blinking suppression and reduction in fluorescence lifetime are chemically reversible by flushing the propyl gallate and illuminating the dots with laser light, as discussed in the following section.

We have also performed preliminary concentration studies for this system, which indicate a decrease in the fluorescence lifetime from 21(1) ns down to 4(1) ns with increasing propyl gallate concentration. The shape of this concentration dependence can be fit with a standard adsorption−desorption kinetic model to yield an affinity constant of $K_D \approx 5(1)$ mM. The interesting observation is that this average fluorescence

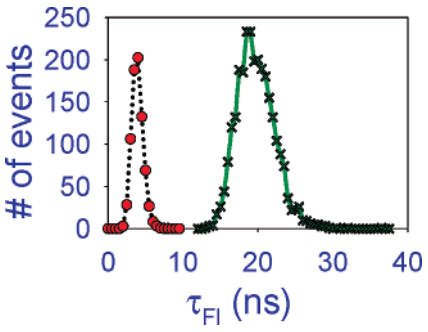

Figure 3. Sample fluorescence lifetime distribution for single CdSe/ZnS core shell quantum dots in the absence (solid line and crosses, $<\tau_{Fl}> = 19(1)$ ns) and presence (dashed line and circles, $<\tau_{Fl}> = 4(1)$ ns) of 12 mM propyl gallate. Because peak count rates and quantum yields ($QY = k_{rad}/(k_{rad} + k_{nonrad}) = k_{rad}\ \tau_{Fl}$) remain constant, the 5-fold decrease in the mean fluorescence lifetime necessarily implies a 5-fold increase in the radiative rate (k_{rad}) due to the solution environment.

lifetime decrease appears to be a smooth, continuous function of concentration. Because we are observing single quantum dots for each measurement, this immediately indicates that the lifetime reduction effect must arise from attachment of substantially more than one propyl gallate ligand, each presumably making incremental contributions to the radiative and nonradiative rates. With the current data, however, it is not possible to say how many total ligands must be involved to achieve the saturation of the lifetime reduction, and therefore the magnitude of contribution provided by a single ligand.

The strong reduction of fluorescent lifetime concomitant with elimination of blinking and yet without reduction in fluorescence quantum yield permits a very simple conclusion. Suppression of blinking by itself could in principle proceed through saturation of trap sites at the quantum dot surface and thus, via the Auger model, systematic elimination of nonradiative channels and a decrease in k_{nonrad}. Indeed, we do see this as the dominant effect for many other chemical blinking suppressants. However, if this were the only factor, the average fluorescence lifetimes would become longer rather than shorter, as evident from the expression $\tau_{FL} = 1/(k_{rad} + k_{nonrad})$. Furthermore, the key observation is that reduction in fluorescence lifetime occurs with no change in peak signal intensities and thus peak quantum yields. Insertion of τ_{Fl} into the defining expression for quantum yield (QY) results in $QY = k_{rad}/(k_{rad} + k_{nonrad}) = \tau_{Fl}k_{rad}$, which leads immediately leads to the conclusion that the 5-fold reduction in τ_{Fl} is accompanied by a nearly 5-fold increase in the radiative rate, k_{rad}. Such environmental manipulation of both radiative and nonradiative rates is reminiscent of the "metal-enhanced fluorescence" results of Lakowicz and coworkers, as well as the strongly accelerated fluorescence emission rates for CdSe quantum dots on roughened metal surfaces by Shimizu et al.[35−38]

From a more quantitative perspective, consider the sample quantum dot data in Figure 1, which yields an average intensity during "on" events of 50(4) and 52(6) KHz, respectively, in the absence and presence of propyl gallate solution. Analysis of the corresponding MLE trajectories yields $<\tau_{Fl}> = 19.5 \pm 3.1$ and 3.9 ± 0.8 ns. On the basis of FCS measurements of the absolute microscope collection efficiency, if we take 50(4) KHz to correspond to a quantum yield of QY = 0.80, then the radiative and noradiative lifetimes would be $\tau_{rad} = 24.4 \pm 3.9$ ns and $\tau_{nonrad} = 100 \pm 100$ ns (without propyl gallate) and $\tau_{rad} = 4.7 \pm 1.0$ ns and $\tau_{nonrad} = 22.9 \pm 30$ ns (with propyl gallate). In each case, the nonradiative component is uncertain to approximately within its own magnitude, while the radiative lifetime is reasonably well extracted and exhibits the aforementioned 5-fold decrease. This does not rule out propyl gallate-induced changes in the nonradiative rate as well. Indeed, the dynamic range of the bright versus dark quantum yields under normal blinking conditions (if ascribed entirely to k_{nonrad}) would correspond to 50−100 fold transient increase in the nonradiative rate, that is, considerably larger than the 5-fold increase observed in k_{rad}. Thus, the presence of propyl gallate must be both inhibiting large transient increases in k_{nonrad} as well as speeding up the intrinsic radiative lifetime. In summary, the data supports an environmental-based sensitivity in both the radiative and nonradiative rates.

Discussion. The microfluidic control of the solution environment readily permits a simple kinetic investigation for recovery of the fluorescence lifetimes and blinking behavior. To achieve this, quantum dots are tethered to a cover glass and inoculated in propyl gallate, flushed thoroughly in situ with plain buffer to remove all excess ligands in solution, and then sampled for fluorescence activity as a function of time. Recovery to the initial blinking state is fully reversible and complete within minutes of illumination. However, to isolate processes that occur in the dark from those that are activated by laser excitation, the studies then proceed in two different ways. First, by taking fluorescence trajectories for dots in a low duty cycle window (<5 s) as a function of time delay after flushing, we obtain "dark" fluorescence lifetime histogram data such as shown in Figure 4. The results indicate only a slight broadening of the fluorescence lifetimes on time scales up to 10 min with discernible shifts in the peak values noted only on time scales of 100 min or longer. The trend indicates recovery in the dark to the initial fluorescence lifetime behavior ($<\tau_{Fl}> = 21(1)$ ns, denoted by the arrow in Figure 4) to be very slow, requiring time scales in excess of several hours. This would be consistent, for example, with strong binding of the propyl gallate to trap states on the ZnS shell with slow off-rates ($<10^{-4}$ s^{-1}) for ligand dissolution back into the buffer. Thus, suppression of blinking in these quantum dots by exposure to propyl gallate is a stable and long-lived phenomenon.

Interestingly, the recovery of blinking dynamics in the presence of laser illumination is relatively rapid. Figure 5 displays sample fluorescence trajectories for a single quantum dot in the propyl gallate buffer (top panel) and after flushing (lower panel). The near complete blinking suppression evident at $t = 0$ is rapidly degraded with illumination with average fluorescence lifetimes shifting back from ≈5 to ≈19-(1) ns after only 2 min, that is, nearly the ≈21(1) ns observed initially. The clear difference between dark and illuminated recovery rates suggests that ligand removal is enhanced by

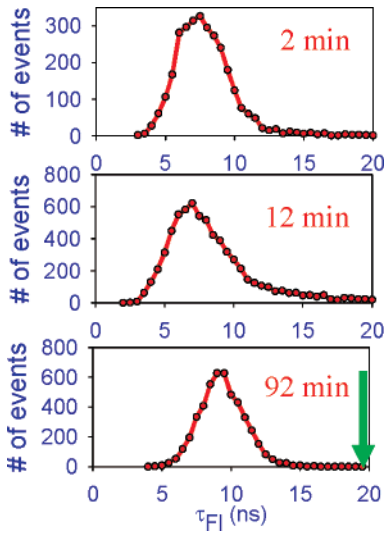

Figure 4. Time dependent recovery of fluorescence lifetimes in the dark. Note the slow recovery toward the untreated fluorescence lifetime (green arrow at $<\tau_{Fl}> = 19(1)$ ns) in the absence of photoexcitation. Fluorescence lifetime recovery is incomplete even after several hours, which would be consistent with strong binding of propyl gallate to trap states at the QD surface.

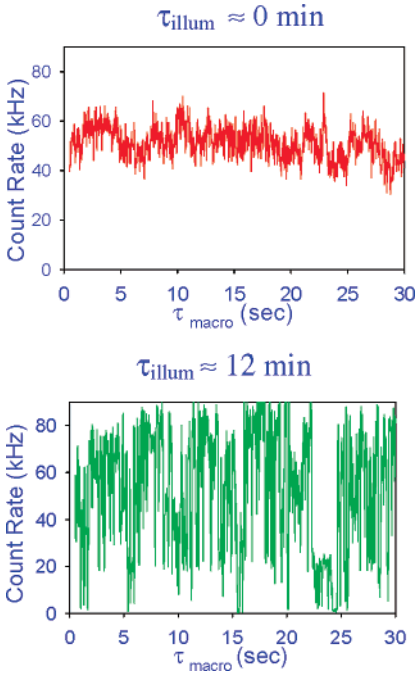

Figure 5. Recovery of quantum dot blinking behavior while under continuous probe illumination (≈100 nW). In contrast to the much slower recovery noted in the dark (see Figure 4), the illuminated quantum dots regain blinking behavior in a matter of several minute (i.e., with $<\tau_{Fl}> \approx 18-22$ ns) This suggests that removal of propyl gallate from surface trap states is promoted by photoexcitation of the dot.

photoexcitation of the quantum dot. On the basis of a linear dependence on number of absorbed photons, the efficiency for such a ligand ejection process is estimated to be of order 10^{-6} or lower. Although this is quite low, this could be consistent with ligand removal from trap states on the surface being linked to rare events such as photoactivated electron (or hole) ejection from the quantum dot core. Further theoretical and experimental work will clearly be necessary to address these issues satisfactorily.

The above time-correlated single photon counting results provide direct evidence for dramatic changes in fluorescence lifetime dynamics of quantum dots based on solution exposure to simple ligands. Although this work explicitly focuses on data for propyl gallate, we have seen similar shifts in CdSe/ZnS nanocrystal quantum yields and fluorescence lifetime data with other chemical species. Thus, there is reason to believe this could be a relatively general phenomenon. Large fluctuations in nonradiative rates for quantum dot electron−hole pair excitation are not unexpected, and based on the Auger model arise from the transient charging of surface trap states due to electron or hole ejection/recombination from the CdSe core. Suppression of quantum dot blinking by environmental passivation of surface trap states to block such events is therefore a plausible consequence of the model. What is more fundamentally surprising is that the radiative rate in quantum dots can be similarly influenced by the presence of surface ligands. At the current time, we are not ready to commit to a single definitive mechanism for such a phenomenon. We can, however, offer the following thoughts for further exploration.

As clearly described by Efros,[7] the excited energy level structure for quantum dots is best described in terms of a dark/bright exciton model.[1,6,7] For a spherically symmetric nanocrystal with a cubic lattice structure, the first exciton state ($1S_{3/2}1S_e$) is 8-fold degenerate with 2- and 4-fold degeneracies arising from the electron and hole, respectively. In real nanocrystal systems, this degeneracy is broken by a combination of electron−hole exchange interaction, crystal shape asymmetry, and lattice structural effects, which have been worked out for a variety of limiting cases.[7] In general, the analysis predicts 5 different states with well-defined projections (F) of total angular momentum along the crystal axis: two nondegenerate states with $F = 0$, two doubly degenerate states with $F = \pm 1$ and one doubly degenerate state with $F = \pm 2$. The $F = 0, \pm 2$ angular momentum states are not optically coupled to the ground state and thus represent dark excitons. The $F = \pm 2$ dark exciton is nominally the lowest exciton state with splittings on the order of 0−50 meV with respect to the $F = \pm 1$ bright and $F = 0$ dark exciton states that depend on specifics of the crystal shape and size. Such a model nicely explains the extremely long fluorescence lifetimes (≈1000 ns) observed in CdSe nanocrystals under low-temperature conditions[53] as arising from relaxation into the ground dark exciton state, as well as the temperature based increase in fluorescence rate due to finite thermal population of lowest $F = \pm 1$ bright exciton state.

The $F = \pm 2$ dark exciton is predicted to be the lowest exciton state for a wide variety of crystal asymmetries and sizes.[7] However, this model does not include the influence of surface trap states and the presence of ligands. One possible explanation for the increase in radiative lifetime in the presence of propyl gallate, therefore, would be if the presence of trap states, surface defects, and/or ligands were able to invert this energy ordering and thereby lead to

preferential thermal population of the bright exciton state. Another possible model could be based on the presence of unpaired electron spins from surface dangling bonds, whose magnetic fields could result in strong coupling between the $F = 0, \pm 2$ dark and $F = \pm 1$ bright exciton levels. It is worth noting that the oscillator strength for bright exciton optical coupling with the ground state in CdSe is predicted[7] to yield a lifetime of order $\tau_{rad} = 1.5$ ns. Thus the enhanced fluorescence lifetimes ($\tau_{rad} = 4(1)$ ns) observed in propyl gallate inoculated CdSe/ZnS nanocrystals would not necessarily require explicit reversal of the dark and bright exciton energy levels but could also be consistent with partial mixing of bright character into the dark exciton. Clearly, more theoretical and experimental effort will be required to establish or refute the validity of such a model.

Summary. In summary, we have shown that controlling the solution chemical environment can lead to quenching of the quantum dot blinking dynamics by influencing both the radiative and nonradiative lifetimes. The important role of time dependent fluctuations in the nonradiative pathway is a natural extension of the Efros and Rosen model for blinking, corresponding to fluctuations in the charge state and therefore Auger relaxation rates of the dot.[3,5] By detailed trajectory analysis of the fluorescence lifetimes and quantum yields, this work highlights the more surprising role of fluctuations in the radiative rate for quantum dots. Specifically, we report a 5-fold increase in the fluorescence rate for room temperature dots inoculated with propyl gallate solution, which for no change in the average peak quantum yields immediately translates into a 5-fold increase in the radiative rate. This also indicates a novel alternative mechanism for blinking suppression, namely by enhanced competition between radiative and nonradadiative pathways. The mechanism for such a radiative lifetime sensitivity to the solution-phase environment is currently not well understood, but one can speculate that ligand-induced shifts in energies of the dark and bright exciton states play a key role.[7] If this is the case, this mechanism predicts a strong temperature dependence to the fluorescence lifetimes, which would be an interesting avenue of investigation. Further theoretical and experimental work will clearly be required to elucidate this intriguing phenomenon. Our experimental results indicate quantum dot blinking dynamics in solution to be considerably richer than previously expected and that blinking suppression cannot be simply attributed to removal of nonradiative relaxation pathways.

As a final comment, there is evidence that such blinking dynamics extend to considerably faster and slower times.[44] Inspection of Figure 2 reveals highly statistically significant fluctuations in nanocrystal fluorescence lifetimes, substantially broader than uncertainties ($\approx$1 ns) from the MLE fits and indicating lifetime fluctuations on time scales faster than 1 ms. Indeed, we have extended studies that reveal the presence of quantum yield fluctuations in single quantum dots on time scales down to 100 ns, as well as slow quantum yield fluctuations on time scales out to 1000 s. Thus, the fundamental physical issues associated with quantum dot fluorescence intermittency would appear to have contributions spanning >10 orders of dynamic range. These investigations into short and long time scale blinking dynamics will be reported elsewhere.

Acknowledgment. We acknowledge the National Science Foundation and the National Institute for Standards and Technology for research support. We also thank Dr. A. L. Efros, Dr. V. Klimov, and Professor R. A. Marcus for their long time supportive interactions and many stimulating discussions.

References

(1) Efros, A. L.; Rosen, M.; Kuno, M.; Nirmal, M.; Norris, D. J.; Bawendi, M. *Phys. Rev. B* **1996**, *54*, 4843.
(2) Chepic, D. I.; Efros, A. L.; Ekimov, A. I.; Vanov, M. G.; Kharchenko, V. A.; Kudriavtsev, I. A.; Yazeva, T. V. *J. Lumin.* **1990**, *47*, 113.
(3) Efros, A. L.; Rosen, M. *Ann. Rev. Mat. Sci.* **2000**, *30*, 475.
(4) Norris, D. J.; Efros, A. L.; Rosen, M.; Bawendi, M. G. *Phys. Rev. B* **1996**, *53*, 16347.
(5) Efros, A. L.; Rosen, M. *Phys. Rev. Lett.* **1997**, *78*, 1110.
(6) Nirmal, M.; Norris, D. J.; Kuno, M.; Bawendi, M. G.; Efros, A. L.; Rosen, M. *Phys. Rev. Lett.* **1995**, *75*, 3728.
(7) Efros, A. L. *Fine Structure and Polarization Properties of Band-Edge Excitons in Semiconductor Nanocrystals*; Marcel Dekker, Inc: New York, 2003.
(8) Malko, A. V.; Mikhailovsky, A. A.; Petruska, M. A.; Hollingsworth, J. A.; Klimov, V. I. *J. Phys. Chem. B* **2004**, *108*, 5250.
(9) Jeong, S.; Achermann, M.; Nanda, J.; Lvanov, S.; Klimov, V. I.; Hollingsworth, J. A. *J. Am. Chem. Soc.* **2005**, *127*, 10126.
(10) Hohng, S.; Ha, T. *J. Am. Chem. Soc.* **2004**, *126*, 1324.
(11) Murray, C. B.; Nirmal, M.; Norris, D. J.; Bawendi, M. G. *Z. Phys. D: At., Mol. Clusters* **1993**, *26*, S231.
(12) Murray, C. B.; Norris, D. J.; Bawendi, M. G. *J. Am. Chem. Soc.* **1993**, *115*, 8706.
(13) Norris, D. J.; Nirmal, M.; Murray, C. B.; Sacra, A.; Bawendi, M. G. *Z. Phys. D: At., Mol. Clusters* **1993**, *26*, 355.
(14) Danek, M.; Jensen, K. F.; Murray, C. B.; Bawendi, M. G. *Chem. Mater.* **1996**, *8*, 173.
(15) Alivisatos, A. P. *Science* **1996**, *271*, 933.
(16) Manna, L.; Scher, E. C.; Alivisatos, A. P. *J. Am. Chem. Soc.* **2000**, *122*, 12700.
(17) Peng, X. G.; Manna, L.; Yang, W. D.; Wickham, J.; Scher, E.; Kadavanich, A.; Alivisatos, A. P. *Nature* **2000**, *404*, 59.
(18) Schaller, R. D.; Petruska, M. A.; Klimov, V. I. *J. Phys. Chem. B* **2003**, *107*, 13765.
(19) Wehrenberg, B. L.; Wang, C. J.; Guyot-Sionnest, P. *J. Phys. Chem. B* **2002**, *106*, 10634.
(20) Hines, M. A.; Guyot-Sionnest, P. *J. Phys. Chem. B* **1998**, *102*, 3655.
(21) Peterson, J. J.; Krauss, T. D. *Nano Lett.* **2006**, *6*, 510.
(22) Du, H.; Chen, C. L.; Krishnan, R.; Krauss, T. D.; Harbold, J. M.; Wise, F. W.; Thomas, M. G.; Silcox, J. *Nano Lett.* **2002**, *2*, 1321.
(23) Krauss, T. D.; Brus, L. E. *Phys. Rev. Lett.* **1999**, *83*, 4840.
(24) Banin, U.; Bruchez, M.; Alivisatos, A. P.; Ha, T.; Weiss, S.; Chemla, D. S. *J. Chem. Phys.* **1999**, *110*, 1195.
(25) Basche, T. *J. Lumin.* **1998**, *76*−*7*, 263.
(26) Nirmal, M.; Dabbousi, B. O.; Bawendi, M. G.; Macklin, J. J.; Trautman, J. K.; Harris, T. D.; Brus, L. E. *Nature* **1996**, *383*, 802.
(27) Empedocles, S. A.; Bawendi, M. G. *J. Phys. Chem. B* **1999**, *103*, 1826.
(28) Empedocles, S. A.; Bawendi, M. G. *Science* **1997**, *278*, 2114.
(29) Empedocles, S. A.; Norris, D. J.; Bawendi, M. G. *Phys. Rev. Lett.* **1996**, *77*, 3873.
(30) Neuhauser, R. G.; Shimizu, K. T.; Woo, W. K.; Empedocles, S. A.; Bawendi, M. G. *Phys. Rev. Lett.* **2000**, *85*, 3301.
(31) Verberk, R.; van Oijen, A. M.; Orrit, M. *Phys. Rev. B* **2002**, *66*.
(32) Koberling, F.; Kolb, U.; Philipp, G.; Potapova, I.; Basche, T.; Mews, A. *J. Phys. Chem. B* **2003**, *107*, 7463.
(33) Early, K. T.; McCarthy, K. D.; Hammer, N. I.; Odoi, M. Y.; Tangirala, R.; Emrick, T.; Barnes, M. D. *Nanotechnology* **2007**, *18*.
(34) Hammer, N. I.; Early, K. T.; Sill, K.; Odoi, M. Y.; Emrick, T.; Barnes, M. D. *J. Phys. Chem. B* **2006**, *110*, 14167.
(35) Shimizu, K. T.; Woo, W. K.; Fisher, B. R.; Eisler, H. J.; Bawendi, M. G. *Phys. Rev. Lett.* **2002**, *89*.
(36) Ray, K.; Chowdhury, M. H.; Lakowicz, J. R. *Anal. Chem.* **2007**, *79*, 6480.

(37) Lakowicz, J. R. *Anal. Biochem.* **2005**, *337*, 171.
(38) Geddes, C. D.; Lakowicz, J. R. *J. Fluoresc.* **2002**, *12*, 121.
(39) Koberling, F.; Mews, A.; Basche, T. *Adv. Materials* **2001**, *13*, 672.
(40) Pistol, M. E.; Castrillo, P.; Hessman, D.; Prieto, J. A.; Samuelson, L. *Phys. Rev. B* **1999**, *59*, 10725.
(41) Equipment manufacturer identification is solely intended to provide additional information to the reader and does not represent any specific endorsement by the National Institute for Standards and Technology.
(42) Kuno, M.; Fromm, D. P.; Hamann, H. F.; Gallagher, A.; Nesbitt, D. J. *J. Chem. Phys.* **2001**, *115*, 1028.
(43) Kuno, M.; Fromm, D. P.; Hamann, H. F.; Gallagher, A.; Nesbitt, D. J. *J. Chem. Phys.* **2000**, *112*, 3117.
(44) Biebricher, A.; Sauer, M.; Tinnefeld, P. *J. Phys. Chem. B* **2006**, *110*, 5174.
(45) Kapitonov, A. M.; Stupak, A. P.; Gaponenko, S. V.; Petrov, E. P.; Rogach, A. L.; Eychmuller, A. *J. Phys. Chem. B* **1999**, *103*, 10109.
(46) Schwille, P. *Fluorescence Correlation Spectroscopy: Theory and Applications*; Springer: Berlin, 2001.
(47) Hess, S. T.; Huang, S. H.; Heikal, A. A.; Webb, W. W. *Biochemistry* **2002**, *41*, 697.
(48) Widengren, J.; Mets, U.; Rigler, R. *J. Phys. Chem.* **1995**, *99*, 13368.
(49) Harada, Y.; Sakurada, K.; Aoki, T.; Thomas, D. D.; Yanagida, T. *J. Mol. Biol.* **1990**, *216*, 49.
(50) Tellinghuisen, J. *Anal. Chem.* **1993**, *65*, 1277.
(51) Tellinghuisen, J.; Goodwin, P. M.; Ambrose, W. P.; Martin, J. C.; Keller, R. A. *Anal. Chem.* **1994**, *66*, 64.
(52) Tellinghuisen, J.; Wilkerson, C. W. *Anal. Chem.* **1993**, *65*, 1240.
(53) Bawendi, M. G.; Wilson, W. L.; Rothberg, L.; Carroll, P. J.; Jedju, T. M.; Steigerwald, M. L.; Brus, L. E. *Phys. Rev. Lett.* **1990**, *65*, 1623.

NL0726609